AD NUMBER

AD484962

NEW LIMITATION CHANGE

TO

Approved for public release, distribution unlimited

FROM

Distribution authorized to U.S. Gov't. agencies and their contractors; Administrative/Operational Use; JAN 1966. Other requests shall be referred to Office of Naval Research, Arlington, VAB 22203.

AUTHORITY

ONR ltr, 12 Dec 1975

AD No._____

UNCLASSIFIED

484362

NAVSO P-970

REPRINTED FROM

U.S. NAVY JOURNAL of

UNDERWATER ACOUSTICS

Volume 16, No. 2

April 1966

UNCLASSIFIED

When this article is referenced in unclassified reports or articles or listed in unclassified bibliographies (except TAB), indexes, etc., the citation should give the author and title followed by: In "Unpublished Report," Office of Naval Research, Code 468, and date (month and year) of the particular issue involved.

UNDERWATER SOUND IN THE ARCTIC OCEAN*

R. H. Mellen

AVCO Corporation
Marine Electronics Office
New London, Connecticut

ABSTRACT

From 1958 to 1962 the U.S. Navy Underwater Sound Laboratory carried on an experimental program to investigate underwater acoustics in the Arctic Ocean. The results of this program are contained in a report entitled "Underwater Sound in the Arctic Ocean"[1] which is now in the process of publication. This article summarizes that report.

INTRODUCTION

The three major areas investigated were propagation loss, surface reverberation, and ambient noise. Propagation loss measurements were made between several of the drift stations occupied during that period. Aircraft were also employed to drop charges along various tracks covering most of the Canadian Basin. Reverberation and ambient noise measurements were made at the drift stations independently.

PROPAGATION

In the Arctic Ocean the speed of sound usually increases with depth. Figure 1 is a typical sound speed depth profile. Propagation can be described by rays that are refracted upward and suffer repeated reflection at the surface. At long range the deep rays arrive first. As time progresses the ray depth decreases while the rate of arrival increases. Graphic recordings of signatures received at 800 km from shots ranging in size from 1 to 375 pounds are shown in Fig. 2. Since all other conditions were the same, it is evident that the differences in these signatures depend mainly on the source characteristics, i.e., on the relative frequency content and the bubble pulse frequency.

Typical Vibralyzer (frequency vs time) recordings of two shot signatures are shown in Fig. 3. Here it is more obvious that the basic arrival rate (which is related to the fundamental frequency of normal mode theory) increases with time. Two or three modal harmonics are also quite evident. Bubble pulse interference effects appear as amplitude modulation of the traces at multiples of the bubble pulse frequency.

Perhaps the most striking features of Figs. 2 and 3 are the abrupt onset and termination of the signatures. In some cases the onset may be governed by the bottom-limited ray. In other cases, however, we find that the water depth over the entire transmission path is greater than

*This paper was originally presented at the Arctic Acoustics Symposium sponsored by the Office of Naval Research at GM Defense Research Laboratories, Santa Barbara, California on 4-5 January 1966.

[1]R. H. Mellen and H. W. Marsh, "Underwater Sound in the Arctic Ocean," AVCO/MEO Report submitted to U.S. Navy Underwater Sound Laboratory, New London, Connecticut (Dec. 1965). See also, H. W. Marsh and R. H. Mellen, "Underwater Sound Propagation in the Arctic Ocean," J. Acoust. Soc. Am. 35, 552-563 (1963), and R. H. Mellen and H. W. Marsh, "Underwater Sound Reverberation in the Arctic Ocean," J. Acoust. Soc. Am. 35, 1645-1648 (1963).

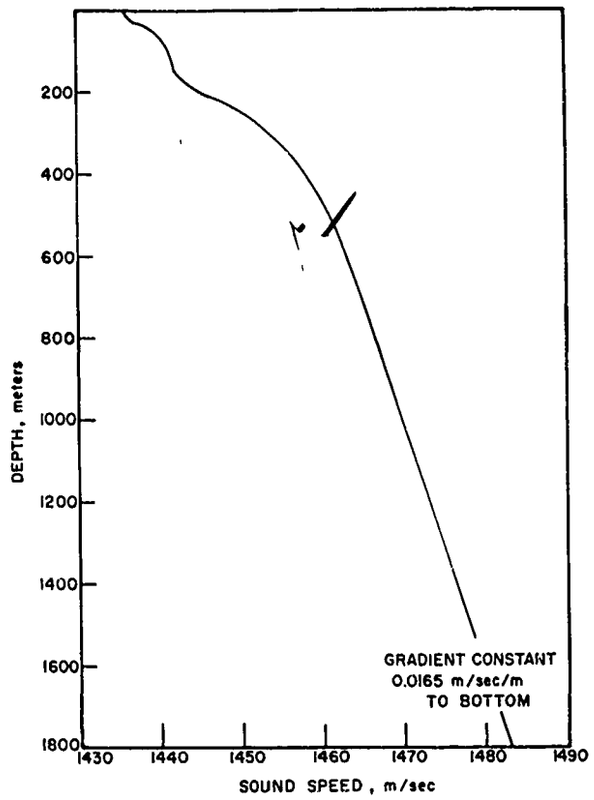

Fig. 1. Sound speed depth profile

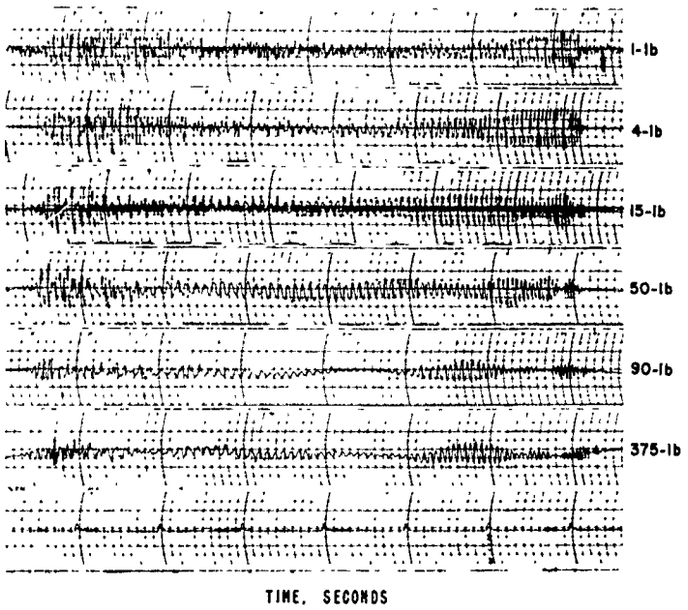

Fig. 2. Shot signature graphic recordings

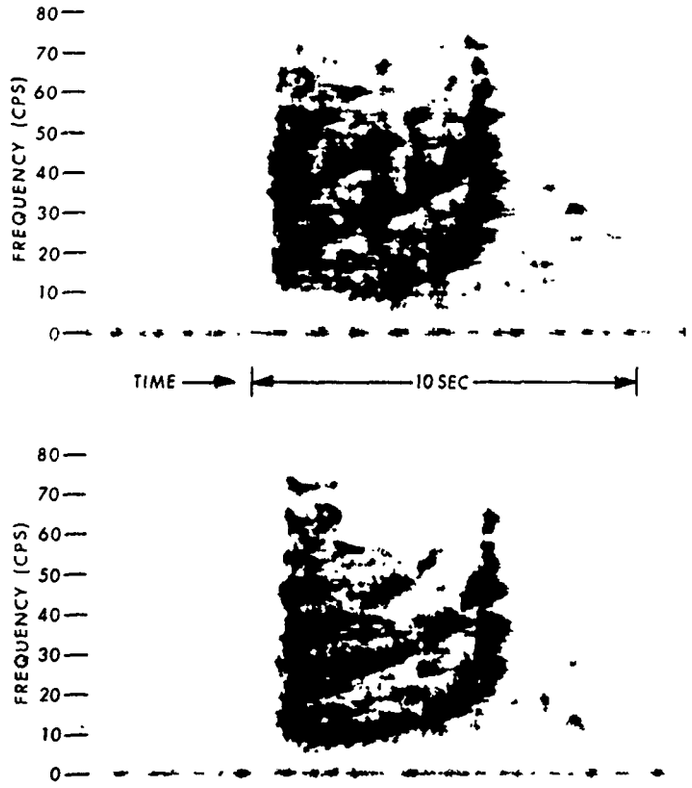

Fig. 3. Shot signature vibralyzer recordings

the vertex depth at onset. We must conclude that the ice cover has a "critical angle" of reflection such that all rays with grazing angles greater than 12 degrees (vertex depth approximately 1 km) are strongly attenuated.

The termination of the shot signature is governed by the sound speed near the surface. In fact, the sound speed profile often causes a group velocity minimum for grazing angles near 7 degrees. The result of these two bounds is a uniform time dispersion of the signal equal to approximately 1 percent of the travel time. Figure 4 shows the signal duration or travel time for some 50 different shots under various conditions.

When the water is shallower than 1 km, the dispersion is less. The upper part of Fig. 5 shows a fairly normal Vibralyzer pattern for a range of 1200 km while the lower part shows the cut-off effect of the bottom. (Chuckchi rise) The normal signal is less than 1 second. Both also show weak bottom reflected modes following the refracted arrival. The upper part of Fig. 6 is an extreme example of bottom reflection in which the refracted arrival is completely obscured. In the lower part the path length is the same, but the bottom path topography has changed so that the bottom-reflected modes disappear.

Another striking feature of the signatures is the absence of high frequencies. This abnormally high attenuation is caused by scattering by the rough ice cover. In our simplified model for transmission loss we have considered only the effects of surface scattering and refraction. Spreading loss is taken as spherical for the first skip zone (about 6 km) and cylindrical beyond that. To this we add the scattering loss per bounce. A comparison of the theoretical and experimental transmission loss vs range for a frequency of 20 Hz is shown in Fig. 7. The experimental data points are identified in the table. The straight line represents spreading loss

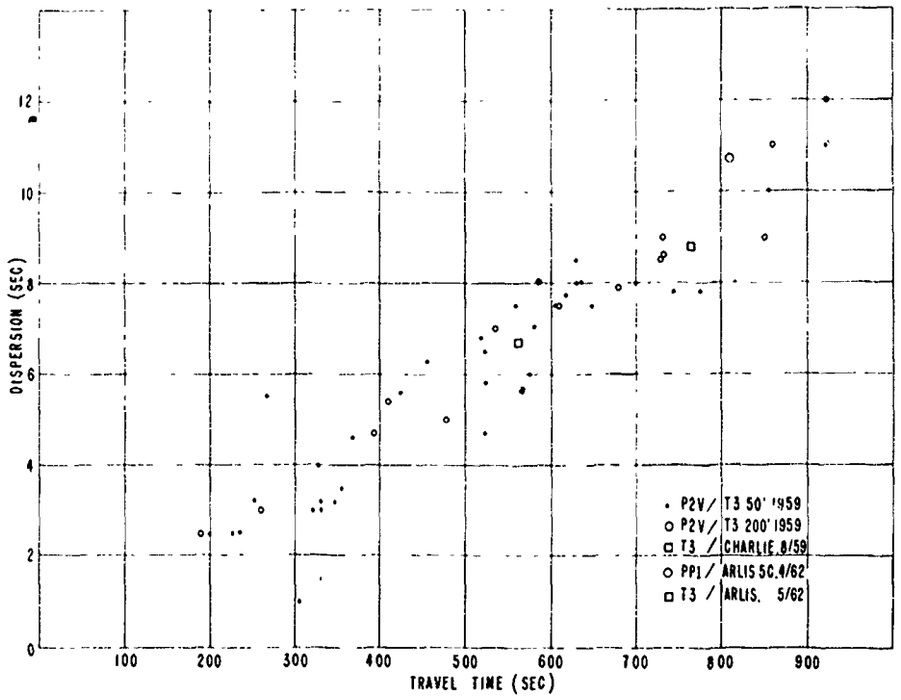

Fig. 4. Shot signature deviation vs travel time

only and the curve S represents the addition of scattering loss. The spread in the experimental values is considerable and represents the combined effects of variation in bottom topography and ice cover as well as experimental error; however in Figs. 8-12 the increase of scattering loss with frequency is quite clearly evident. In Fig. 13 the scattering loss curve (S) has been replaced with absorption loss (A) to show the lower possible limit of transmission loss. Generally the scattering loss approximation is excessive for frequencies above a few hundred Hz, particularly at shorter ranges where the number of surface bounces is small, hence was omitted in Figs. 12 and 13.

It should also be noted that many of the transmission loss values at ranges less than 10 km are abnormally low. This is probably the result of convergence that produces concentration of energy at multiples of the skip distance. At long ranges, however, the zones tend to spread and overlap so that this spreading loss eventually decreases monotonically with range.

REVERBERATION

In fitting the theoretical transmission loss to the experimental points we assumed a random rough surface with an rms height of 2.5 meters. This assumption is supported by reverberation measurements from which the roughness spectrum is deduced directly. The rms roughness is then obtained by integration.

Figure 14 shows a typical frequency analysis of reverberation level vs time from a 100-pound shot received by a hydrophone a short distance away. From these received levels we computed the reverberation strength vs time knowing the source level, and calculating the transmission loss and reverberating area vs time. Finally by calculating the surface grazing angle vs time we deduce roughness/wavenumber spectrum. Figure 15 shows the result of these calculations for some dozen shots of various size. Also shown for comparison is Burling's sea

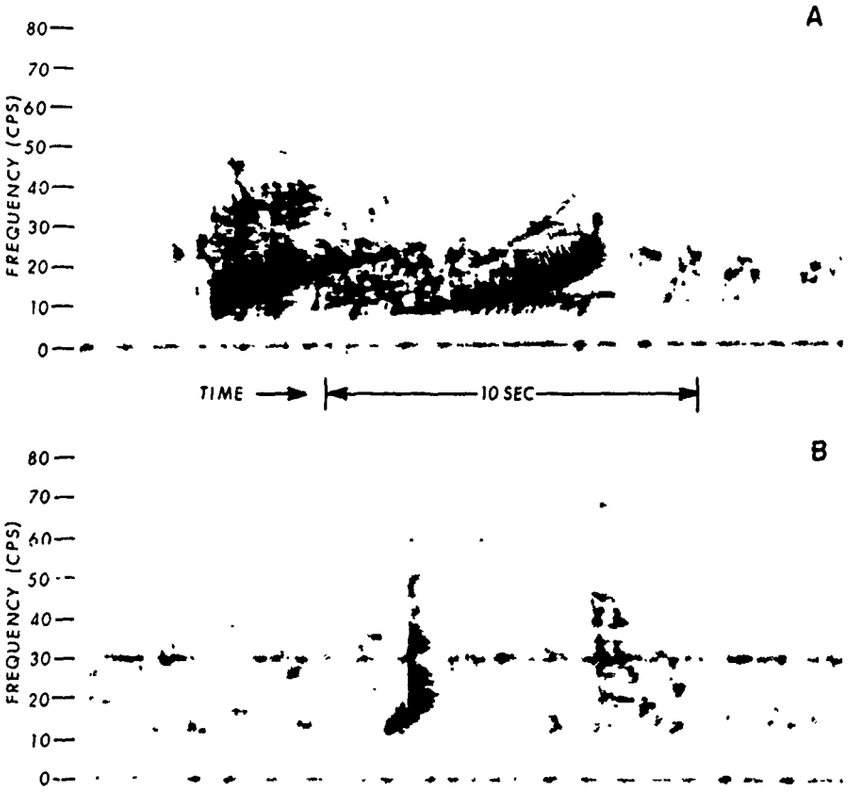

Fig. 5. Vibralyzer recordings, bottom cut-off

surface spectrum which goes as K^{-3}. It is seen that above 2 M^{-1} the curves are roughly parallel, but the ice spectrum is some 40 db higher. Integration of the roughness spectrum gives an rms value of roughness of approximately 3 meters in good agreement with the earlier value. (The standard deviation is about ±5 db)

An additional feature of Fig. 14 is the peak occurring between 40 and 50 seconds. This is no doubt a refraction effect and has been observed on all the shots analyzed. The travel time corresponds to a grazing angle of 16 degrees for the direct ray and 11 degrees for the single bounce. These values are on either side of the 12-degree ray which was noted to be the apparent "critical angle" of reflection.

AMBIENT NOISE

The ambient noise level in the Arctic Ocean is often below the Knudsen sea state zero equivalent. Early attempts at measurement with the PQM hydrophone were frustrated by excessive system noise. In 1961 an improved system was devised using a bilaminar disc hydrophone. Figure 16 shows the system noise of the latter compared to the Knudsen sea state zero spectrum. Also shown are typical noise spectra encountered during the measurement period.

Curve A is an ultraquiet condition with no wind and stable temperature. The peak in the spectrum between 20 and 80 Hz is interpreted to represent noise received from distant sources via the transmission "bandpass."

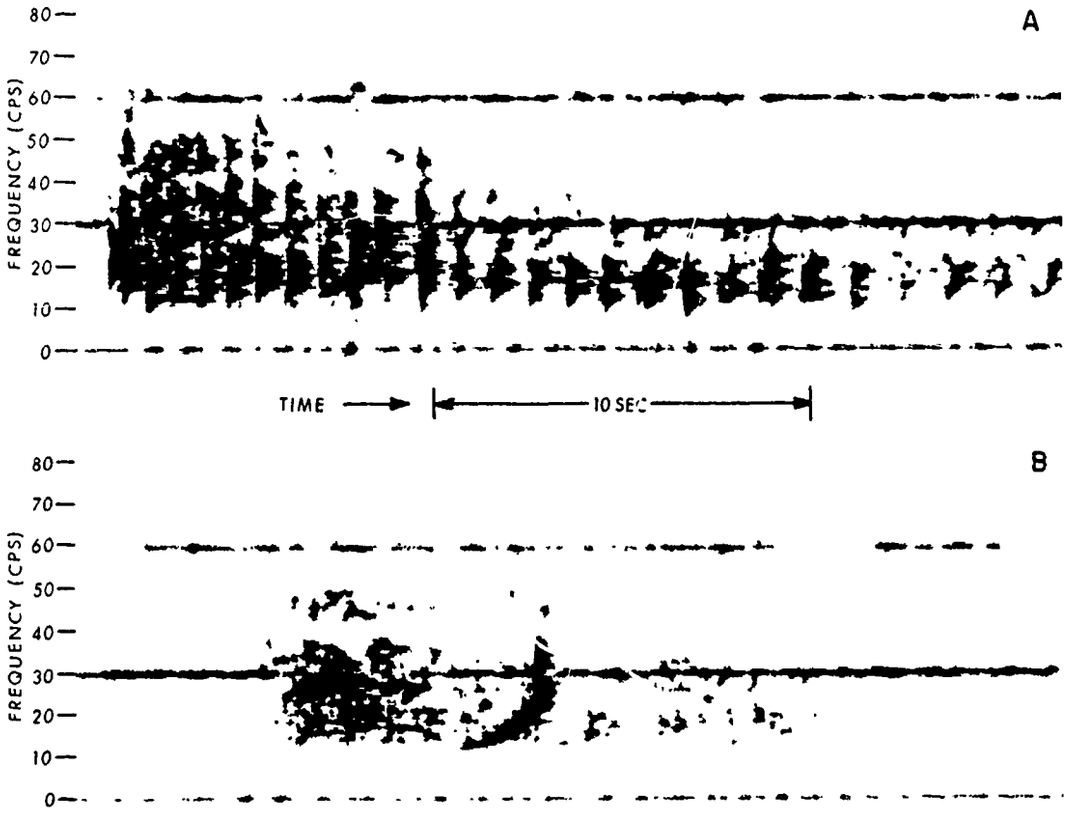

Fig. 6. Vibralyzer recordings, bottom reflections

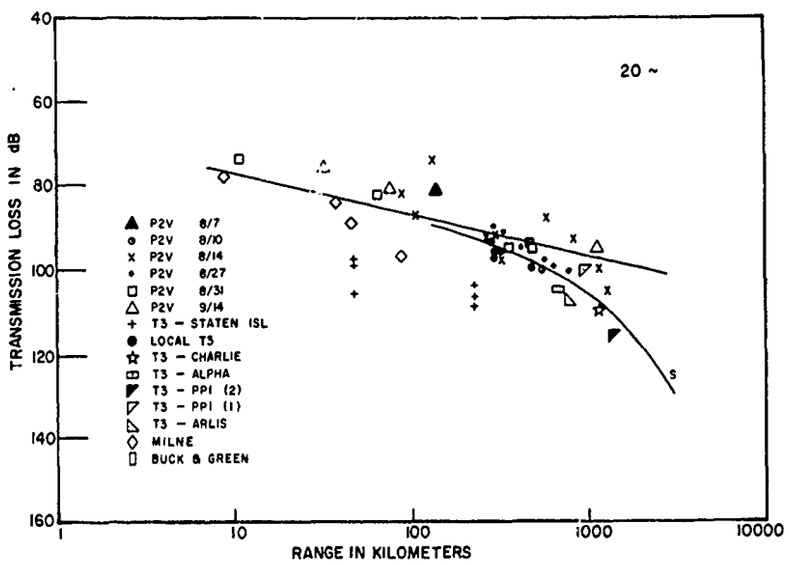

Fig. 7. Transmission loss vs range (20 Hz)

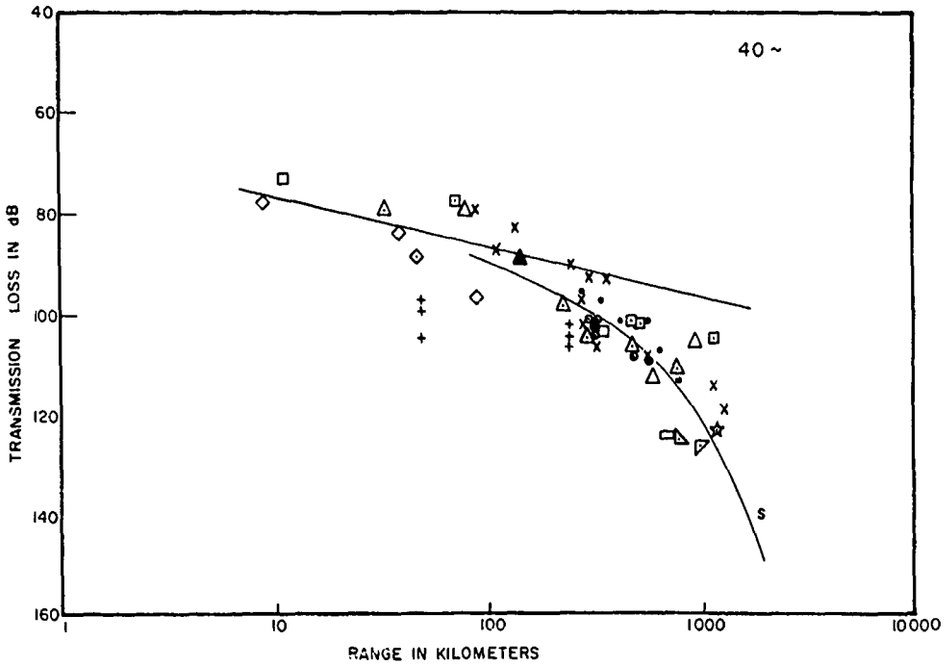

Fig. 8. Transmission loss vs range (40 Hz)

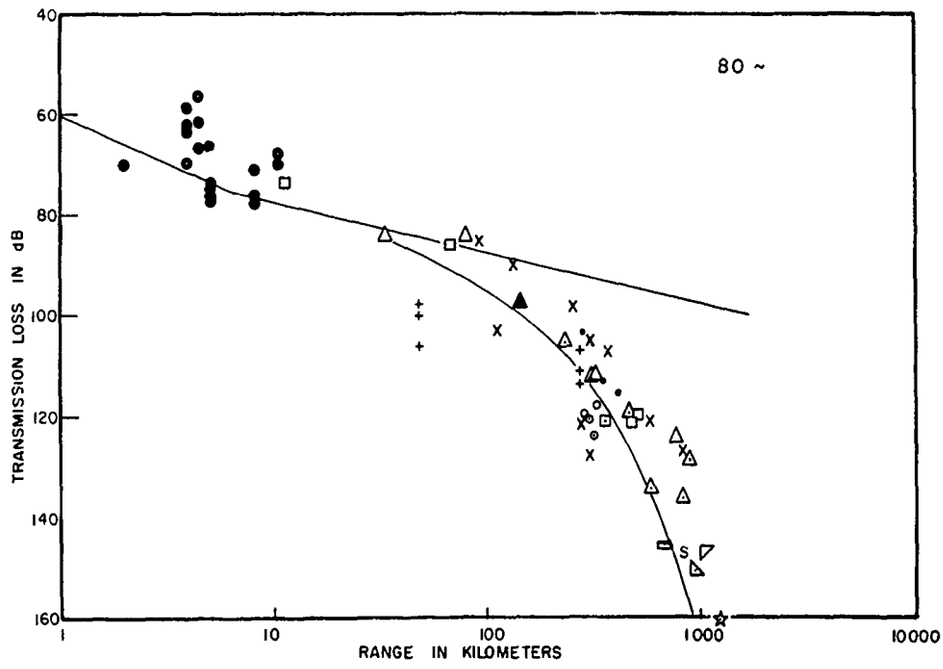

Fig. 9. Transmission loss vs range (80 Hz)

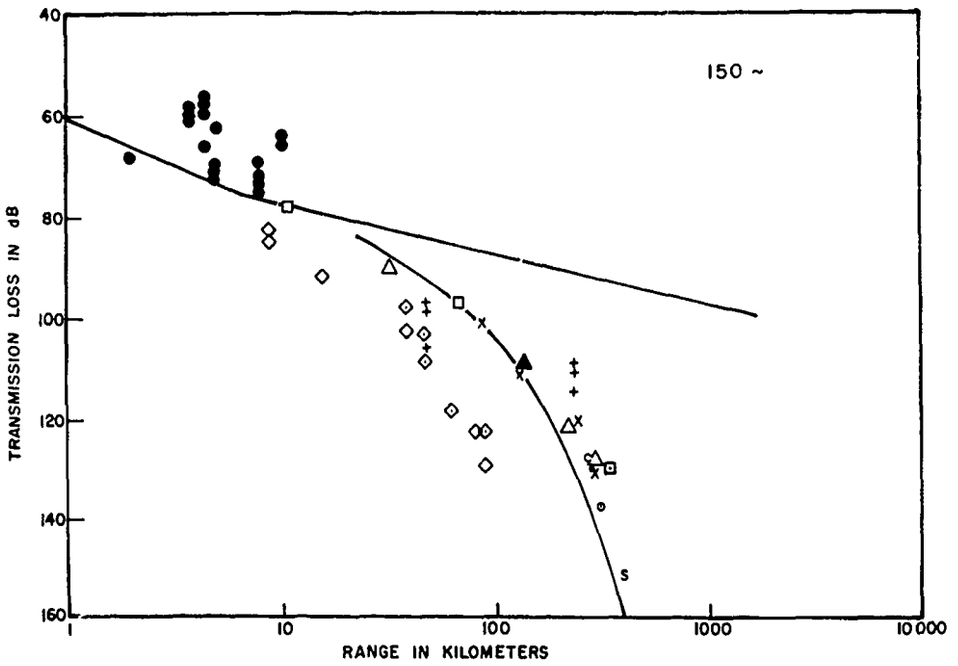

Fig. 10. Transmission loss vs range (150 Hz)

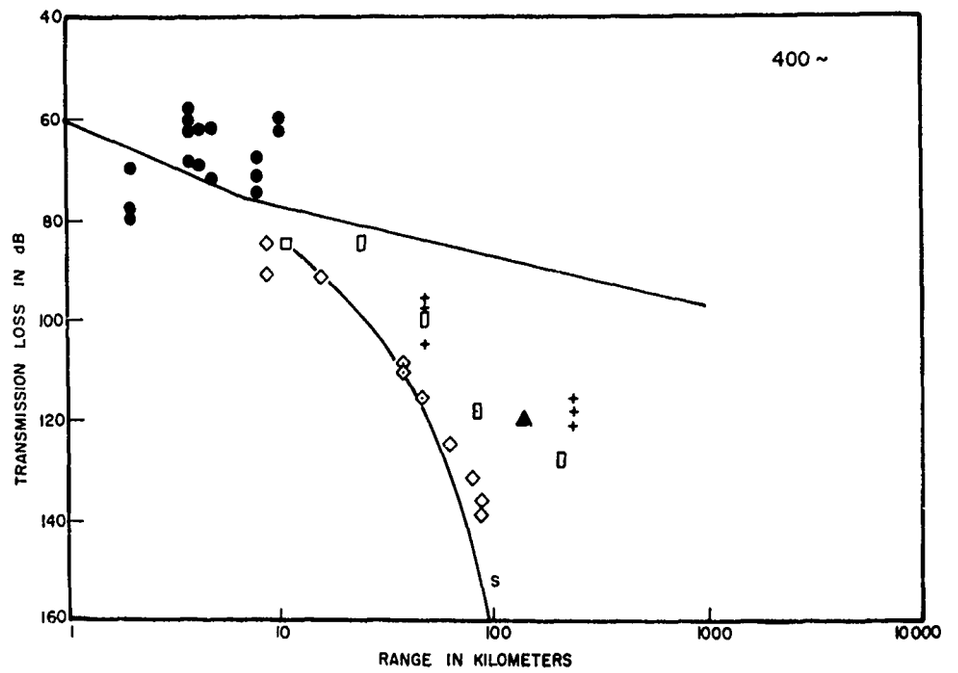

Fig. 11. Transmission loss vs range (400 Hz)

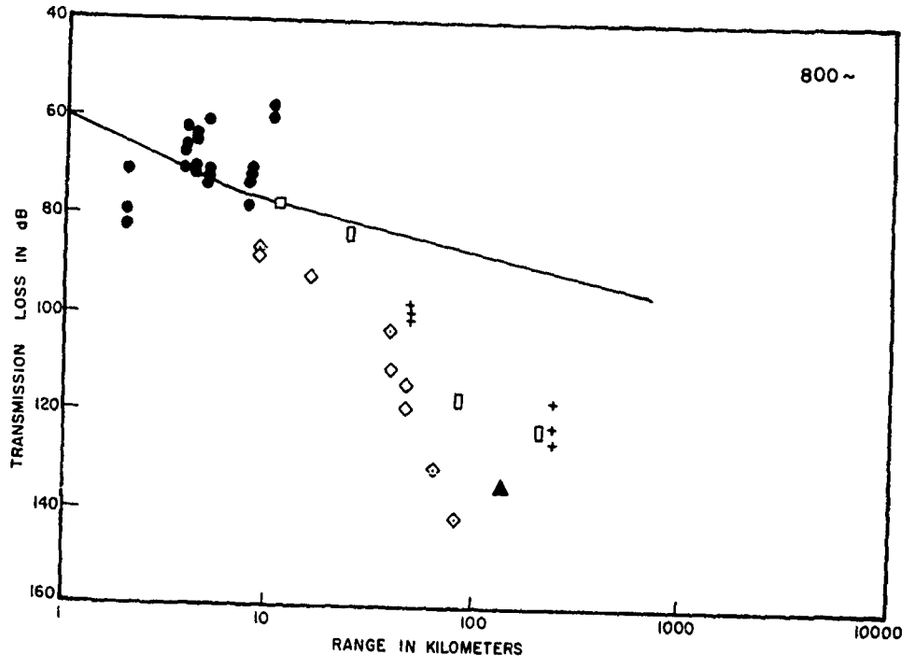

Fig. 12. Transmission loss vs range (800 Hz)

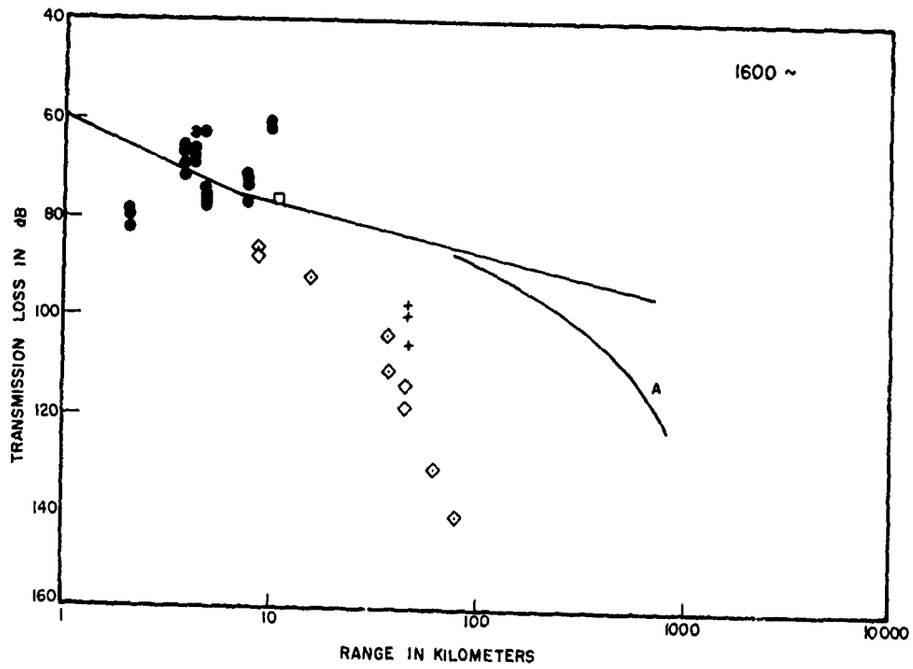

Fig. 13. Transmission loss vs range (1600 Hz)

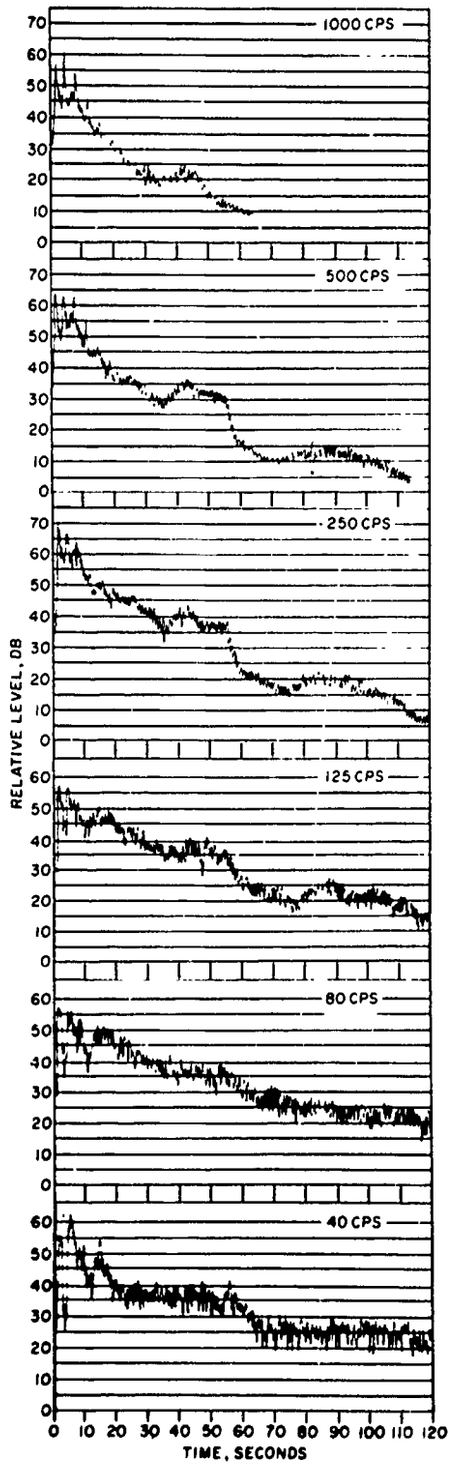

Fig. 14. Reverberation level vs time

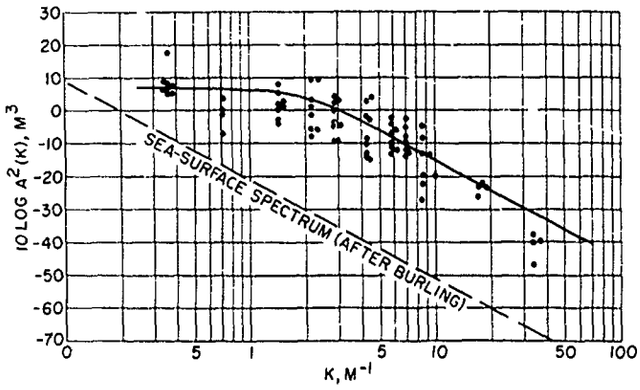

Fig. 15. Ice roughness spectrum

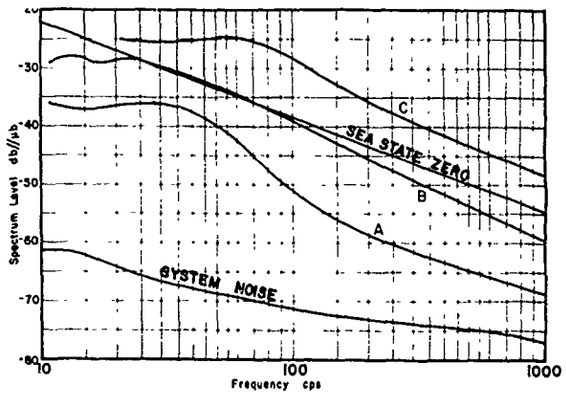

Fig. 16. Ambient noise spectra

Curve B illustrates a condition where the local temperature has dropped suddenly. The ice contracts causing fractures which radiate snapping noises into the water and the ambient noise rises.

Curve C is the maximum level encountered during the period. These curves summarize some 100 ambient noise recordings; however, since camp activities had to be suspended during noise measurements, they are restricted in scope. Also during periods of high winds cable flutter caused by water currents prevented successful measurements. The latter problem was finally solved by using fairing.

The vertical velocity spectra of the ice as measured with a seismometer is compared in Fig. 17, with that inferred from underwater pressure measurements. The vertical velocity of the surface is assumed to be equal to twice the pressure divided by the acoustic impedance of the water. The agreement between the two measurements is interpreted to mean that the ice vibrations are shear and compressional waves of greater speed than that of sound in water so that the coupling between the two media is by direct acoustic radiation (monopole).

During the summer months, sounds are occassionally heard which are obviously of biological origin. Figure 18 shows samples of Vibralyzer recordings of these sounds. Identification of the sources, however, has not yet been successful.

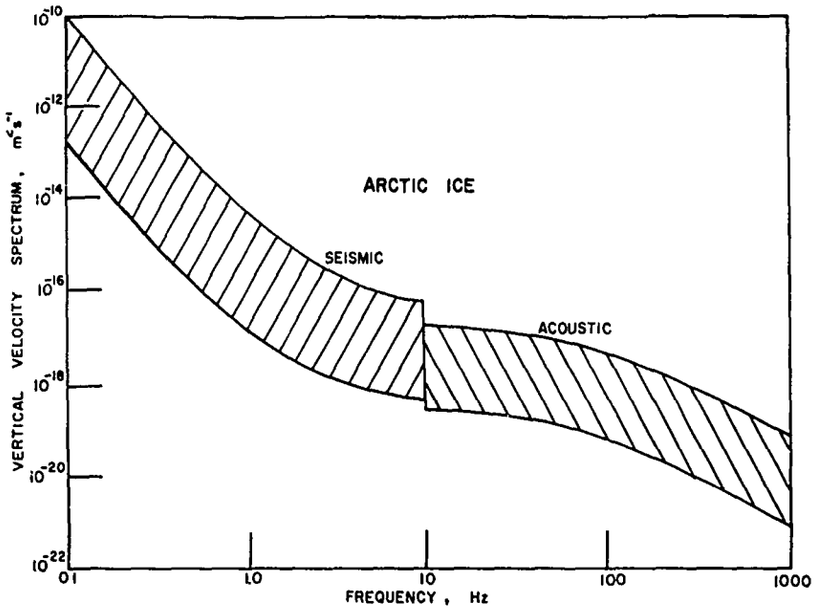

Fig. 17. Ice surface velocity spectra

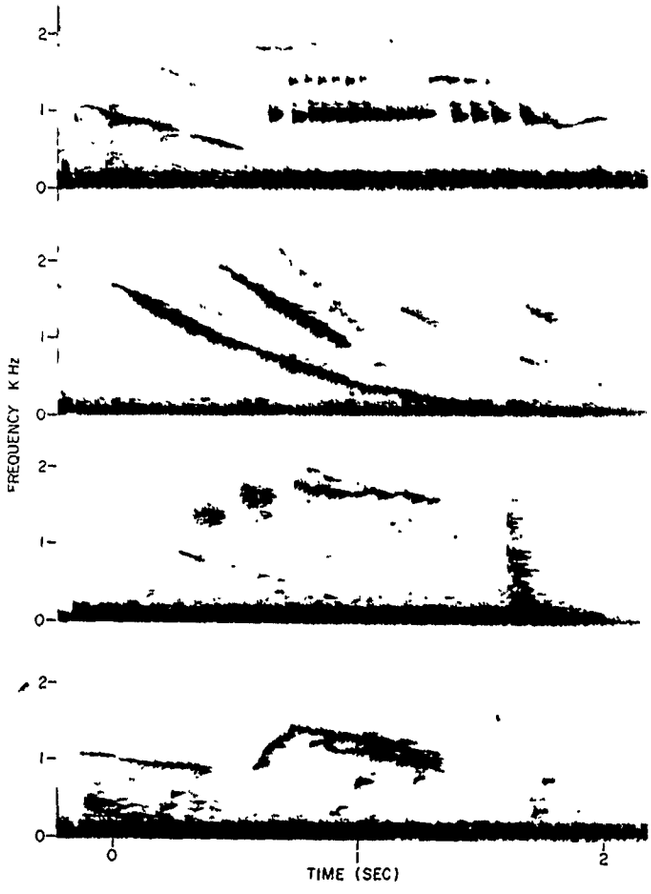

Fig. 18. Biological noise vibralyzer recordings